Acta Cryst. (1996). D52, 1098–1106

The Rate of Water Equilibration in Vapor-Diffusion Crystallizations: Dependence on the Distance from the Droplet to the Reservoir

JOSEPH R. LUFT,[a] DOUGLAS T. ALBRIGHT,[b] JAMES K. BAIRD[b] AND GEORGE T. DETITTA[a]

[a]*Hauptman-Woodward Medical Research Institute, Inc., (formerly the Medical Foundation of Buffalo, Inc.), 73 High Street, Buffalo, New York 14203-1196 USA, and* [b] *University of Alabama in Huntsville, Department of Chemistry, Huntsville, Alabama 35899 USA. E-mail: detitta@hwi.buffalo.edu*

(Received 6 March 1996; accepted 28 May 1996)

Abstract

The rate of water equilibration in hanging-drop vapor-diffusion experiments was studied as a function of the distance separating the hanging drop from the surface of the reservoir solution. Hanging drops of 1.00 *M* NaCl were allowed to partially equilibrate with reservoirs of 2.00 *M* NaCl at room temperature. Over the range of droplet–reservoir distances examined, 7.6–119.4 mm, the larger the distance that separated the droplet and reservoir, the slower the droplet equilibrated with the reservoir. The variation of the rate of equilibration with droplet–reservoir distance was non-linear; the rate was most sensitive to variations in the droplet–reservoir separation at short separations. A mathematical model of the equilibration kinetics was developed that fits the experimental data. The model is based on the assumption that the rate-limiting step in vapor-diffusion equilibration is transit of water across the vapor space. A simple device to vary the rate of water equilibration, and thereby optimize macromolecular crystal growth conditions, is described.

1. Introduction

The hanging-drop method is an important tool for macromolecular crystal growth (McPherson, 1982; Ducruix & Giegé, 1992). In the method a droplet containing the macromolecule and a crystallizing agent is suspended, by surface tension, over a reservoir containing a dehydrating agent. In this closed system equilibration is effected as water, in the form of vapor, leaves the drop, traverses the vapor chamber and enters the reservoir. Concentrations of both the macromolecule and the crystallizing agent increase as water is removed from the droplet, leading to nucleation and crystal growth under favorable circumstances.

The kinetics of water equilibration, that is the rate at which water leaves the droplet, controls the rate at which supersaturating conditions develop, and thus can have a critical effect on the outcome of crystallization experiments. The principal factors determining the kinetics of equilibration in vapor-diffusion experiments have been identified by Boistelle & Astier (1988); Fowlis *et al.* (1988); Mikol, Rodeau & Giegé (1990); and Sibille, Clunie & Baird (1991). These include the temperature, drop size and shape, and the concentrations of crystallizing agent in the droplet and dehydrating agent in the reservoir. Fowlis *et al.* developed a full mathematical treatment of the hanging-drop experiment while Sibille *et al.* developed a similar treatment for vapor diffusion in a Plaas-Link tube (Plaas-Link & Cornier, 1988). Both of those treatments assume that the rate-limiting step in vapor-diffusion equilibration is transit of water across the vapor space. On the other hand, Mikol *et al.* argued that phenomena at air/liquid interfaces, where the droplet and reservoir solutions meet the common vapor space, may play a pivotal role in determining the kinetics of equilibration. Indeed, they presented a few experiments in which the distance between the droplet and reservoir surface was varied, and interpreted those results as suggesting that the droplet–reservoir separation has 'little influence on evaporation rate'. This is a view that is at variance with the models and assumptions of Fowlis *et al.* and Sibille *et al.*, each of which requires a specific dependence of the rate of equilibration on the droplet–reservoir separation.

Here we present evidence that, over the range from 7.6 to 119.4 mm, the rate of equilibration in a hanging-drop experiment depends, in a non-linear fashion, upon the distance separating the droplet and the reservoir. This is in accord with the principal assumption of Fowlis *et al.* and Sibille *et al.* that the rate-limiting step in the equilibration is transit across the vapor space. We will further show that quantitative agreement between our experimental results and predictions made using a modified version of the Sibille *et al.* model is very good. Finally, we will describe a protocol to control the rate of equilibration in hanging-drop crystallizations, with a view toward the improvement of crystal quality.

2. Experiments and results

In each of the experiments to be described, a 24 µl hanging drop of 1.00 *M* NaCl was allowed to partially equilibrate with a reservoir containing 2.00 *M* NaCl. After a specified time the drop was retrieved and analyzed by refractometry to determine its sodium chloride concentration. Each experiment was conducted for a specific length of time and at a fixed value of the droplet to reservoir surface distance. The duration and/or the distance were varied from experiment to experiment. Two large sets of experiments were undertaken. In the first set droplet–reservoir separations ranging from 7.6 to 78.3 mm and equilibration durations from 20 to 121 h were examined. In the second set, separations ranging from 88.9 to 119.4 mm and durations of 120 and 168 h were examined.

Droplet and reservoir solutions were prepared with sodium chloride from Sigma and distilled, deionized (Barnstead NANOpure II; > 17.6 MΩ cm) water. Both stock solutions were prepared in large (liter) volumes to allow all of the experiments in each of the sets to be carried out using the same stocks. Droplets of 1.00 *M* NaCl were taken directly from the droplet stock solution. In particular, droplets were not constituted at the time of their formation by 1:1 dilution of reservoir stock. Fresh droplet and reservoir stock solutions were prepared for each of the two sets of experiments undertaken.

The experimental apparatus is shown in Fig. 1. A standard laboratory test tube [Pyrex, ~13.6 mm inside diameter (ID), ~15.9 mm outside diameter (OD), ~127 mm length, ~17.5 ml volume] acted as the reservoir vessel. Using a steel rule and a simple alignment jig, a scribe mark for liquid level was placed on the outer wall of the test tube. The mark was placed a specified distance down from the top lip of the test tube. Reservoir solution, 2.00 *M* NaCl, was introduced into the tube and adjusted dropwise until the meniscus just touched the scribe mark. Care was taken to prevent droplets of reservoir solution from adhering to the wall of the test tube above the scribe mark.

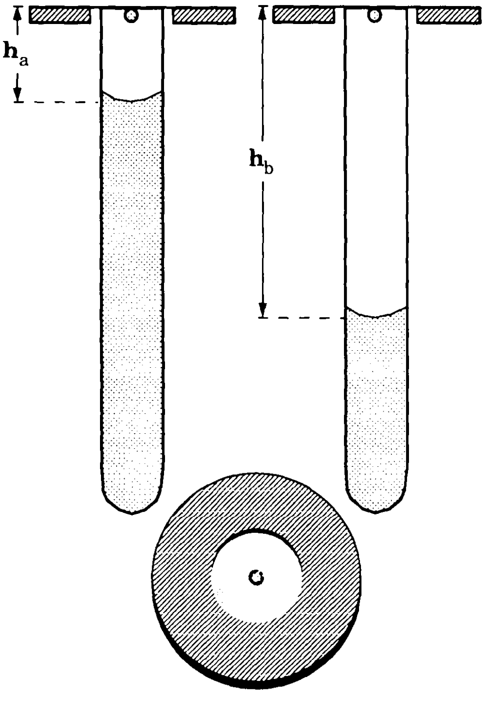

Fig. 1. The experimental arrangement. On the top left and right are two equilibration setups that differ only with respect to the distance from the droplet to the reservoir surface. The droplet is deposited on the adhesive side of clear label tape (bottom), inverted and sealed over the test tubes employed as reservoir vessels. The washer keeps the tape taut and makes manipulation of the droplet quite straightforward, its weight helps to maintain the tape seal, and it acts as a lever to facilitate the recovery of the drop.

Droplets of 1.00 *M* were deposited, using a Gilson Pipetman micropipette set to deliver 24 µl, on the adhesive side of clear plastic label tape (Morris, Kim & McPherson, 1988; Luft & DeTitta, 1992; Luft, Cody & DeTitta, 1992) manufactured by Manco Co. The tape had been affixed to common flat washers (~45 mm OD, ~17 mm ID, ~3 mm thickness, ~34 g). The washers offer firm support for the tape, keeping it taut and allowing for easy manipulation of the drop. The droplet was inverted and immediately sealed over the reservoir, with the tape adhesive making the seal and the weight of the washer helping to maintain it. The establishment of the seal marked the beginning of the partial equilibration. The droplet and reservoir, forming a closed system, were allowed to equilibrate for a specified time, undisturbed and at room temperature (*vide infra*).

Droplets were retrieved by gently prying the tape seal loose, using the washer as a lever. Once the seal was breached the tape could be smoothly peeled away from the rim of the test tube, without fear of losing the droplet. The droplet was pipetted using a Gilson Pipetman and transferred immediately to the prism of a Bausch and Lomb Abbé 3L refractometer where its refractive index was recorded. Using a two-point interpolation scheme in which the refractive indices of the 1.00 and 2.00 *M* NaCl droplet and reservoirs stock solutions were the fixed points, the refractive index of a partially equilibrated droplet was converted into a sodium chloride concentration.

3. The first experimental set

Eleven groups of test tubes, with eight replicate tubes per group, were prepared as described, with varying volumes of reservoir solution surveying 11 values of the droplet–reservoir separation ranging from 7.6 to 78.3 mm. A 12th group, also with eight replicate tubes, was set up with no reservoir solution in the tubes. This 12th group was designed to examine the integrity of the tape seals. The 96 reservoir vessels were prepared well in advance of the start of the equilibrations and were temporarily sealed with double layers of Parafilm to prevent evaporation.

Droplets were applied to fresh tape supports on a schedule of one per minute and sealed over their reservoirs. The equilibrating tubes were held in a rack constructed out of plywood. The rack was housed in double thicknesses of styrofoam to reduce thermal variations over the course of the equilibrations. When the last droplet had been sealed over its reservoir the temperature in the styrofoam box was recorded and the thermal enclosure was sealed. The first 96 experiments were permitted to equilibrate undisturbed for 20 h.

At the end of the equilibration period the thermal enclosure was opened, the temperature recorded, and the droplets were retrieved and analyzed by refractometry as described. The droplets were retrieved in the same order as they were deposited, making it simple to time the 20 h equilibration for each experiment to the minute. As each washer was levered and the drop retrieved the test tube was once again sealed with a fresh double layer of Parafilm.

The same procedures were then followed for equilibration durations of 30, 48, 71, 95, and 121 h. The six subsets of experiments were conducted over the period of one month. The mean temperature of the six equilibrations was 295.9 ± 0.5 K. In 74 out of the total of 963 × 6 = 576 experiments the refractive index measurements indicated that the tape seal had failed. The failure rate, 12.8%, seemed unexpectedly high given our good experience in sealing label tape over Linbro plates (Arakali, Luft & DeTitta, 1995). We noted that ten test tubes, of the 96, were involved in four or more seal failures (out of six equilibration durations) and these tubes accounted for 44 of the 74 failures. Examination of these tubes indicated that each had a small imperfection on the rim where the tape made the seal.

The results of the experiments, including the droplet–reservoir distances, the reservoir volumes, the duration of the equilibrations and the averaged concentrations of NaCl in the droplets, are given in Table 1. The averaged values are for the eight replicates per group with identical droplet–reservoir distances and equilibration duration. Absent from these averaged values are the results from the 74 experiments involving tape-seal failures. Once these were removed there were fewer than eight replicates in some groups, but there were never fewer than four replicate measurements in any group. Thus, it is instructive to note the standard deviations in the averaged NaCl concentrations. Contributions to the standard deviations include the variance of the refractive indices for the droplets in a group and for the calibration measurements using the 1.00 and 2.00 *M* NaCl stock solutions. The standard deviations range from 0.006 to 0.045 *M* NaCl, but the majority of standard deviations are in the range 0.01–0.02 *M* or 1–2% of the range of concentrations expected in the droplets.

Table 1. *Results of the hanging-drop equilibrations versus drop–reservoir distance for the first experimental set*

The starting droplet concentration is 1.0 *M* NaCl and starting volume is 24 µl. The reservoir concentration is 2.0 *M* NaCl. All equilibrations at room temperature 295.9±0.5 K. Each value represents an averaged NaCl concentration (*M*), where the average is over up to eight droplets. The standard deviations are of the average concentration and include contributions from the refractometer calibration as well. Distances (*h*) are measured from the tops of the test tubes to the meniscus of the reservoir solutions. Durations of equilibrium are in h. Volumes (V_{res}) of reservoir solutions are in ml.

Duration (*h*)		20	30	48	71	95	121
				$\langle[\text{NaCl}]^{\text{droplet}}\rangle$ (*M* NaCl)			
h (mm)	V_{res} (ml)						
7.6	16.5	1.48 (1)	1.73 (2)	1.92 (1)	1.97 (1)	2.01 (1)	1.99 (1)
10.2	16.2	1.44 (1)	1.66 (2)	1.88 (2)	1.97 (2)	2.01 (1)	1.99 (1)
15.2	15.6	1.37 (1)	1.59 (1)	1.80 (1)	1.93 (1)	2.00 (1)	1.99 (1)
20.3	15.0	1.30 (1)	1.49 (2)	1.73 (1)	1.87 (2)	1.98 (1)	1.98 (1)
25.4	14.0	1.26 (1)	1.43 (2)	1.65 (1)	1.82 (2)	1.95 (1)	1.96 (1)
38.1	12.4	1.20 (1)	1.33 (1)	1.51 (1)	1.67 (3)	1.87 (1)	1.91 (1)
45.7	11.1	1.18 (2)	1.29 (1)	1.47 (1)	1.59 (1)	1.81 (2)	1.88 (1)
53.3	10.2	1.15 (1)	1.26 (1)	1.41 (1)	1.52 (2)	1.73 (2)	1.81 (1)
61.0	9.2	1.15 (1)	1.23 (1)	1.37 (1)	1.48 (2)	1.67 (1)	1.76 (1)
71.1	7.4	1.13 (1)	1.20 (1)	1.33 (1)	1.41 (2)	1.59 (1)	1.69 (2)
78.3	6.4	1.14 (1)	1.21 (2)	1.32 (1)	1.40 (3)	1.57 (4)	1.67 (5)
–	0	1.04 (1)	1.04 (2)	1.05 (2)	1.03 (1)	1.05 (1)	1.04 (1)

There are two ways in which the results of these experiments can be viewed. In Fig. 2(*a*) the average concentration of NaCl in the droplet is shown as a function of the droplet–reservoir distance, at the six fixed times of the equilibrations. Clearly there is a distance dependence. The closer the droplet is to the reservoir surface, the more fully it has equilibrated with the reservoir for any fixed time. In Fig. 2(*b*) the average concentration of NaCl in the droplet is shown as a function of time, at the 11 fixed droplet–reservoir distances. Also shown in Fig. 2(*b*) are the results from the 12th group of equilibrations, in which droplets were allowed to equilibrate with empty reservoir vessels. As can be seen, these droplets do lose some water to their reservoir vessels. The average concentration of these drops is 1.04 (1) *M* NaCl. Based on a simple gas law calculation, we expect that the droplets will lose ~35 µg of water (from their original volume of 24 µl) and should concentrate to approximately 1.02 *M* NaCl. What we observe is a loss of water about twice what the gas law predicts. Most likely not all of the water lost by the droplets is exchangeable; some is probably bound tightly by the glass wall of the test tube or the adhesive side of the label tape. What is important to observe is that the concentration of NaCl in these droplets is not time dependent, meaning that the tape seal, when properly made, does indeed hold, and that there is no slow leakage of water through the tape over the course of these experiments.

At the conclusion of the first experimental set, the reservoir solutions for the 88 vessels containing reservoir solution were examined by refractometry. Even though the same reservoir solutions had been employed in six equilibrations, there was no evidence that the reservoir concentrations had shifted from 2.00 *M* NaCl. This is not surprising given that the minimum volume of reservoir solution was 6.4 ml. Even if all six of the 24 µl droplets placed over the reservoirs had fully equilibrated, the

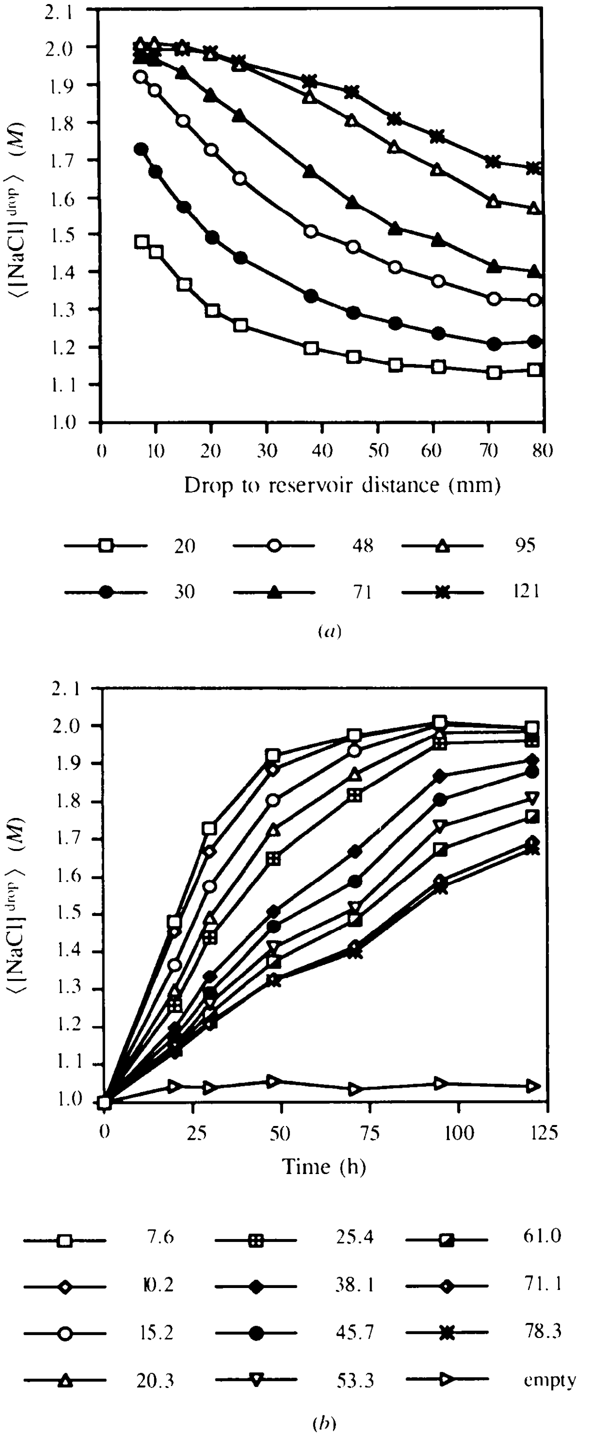

Fig. 2. Results of the first set of equilibration experiments, at 295.9 ± 0.5 K. The droplets are initially 24 µl volume and 1.00 *M* NaCl. The reservoirs are 2.00 *M* NaCl. The average NaCl concentration in the droplet is plotted as a function of (*a*) the droplet-reservoir distance at six equilibration durations (20, 30, . . . , 121 h) and (*b*) the equilibration duration at 11 droplet-reservoir distances (7.6, 10.2, . . . , 78.3 mm). Also shown in (*b*) are the results of the equilibration of 24 µl 1.00 *M* NaCl hanging drops against empty reservoirs.

Table 2. *Results of the hanging-drop equilibrations versus droplet-reservoir distance for the second experimental set*

The experimental details are as in Table 1 except that the room temperature was 297.4±0.5 K. Values in the last two columns are for the 120 h equilibration, first corrected to 121 h to coincide with the 121 h experiment described in the first experimental set, and then further corrected to the temperature of the first experimental set. See text for the descriptions of the corrections. The quotation marks indicate the corrected conditions (duration, temperature).

	Duration (h)	120	168	'121'	'121'
	Temperature (K)	297.2	297.2	297.2	'295.7'
h (mm)	$V_{\rm res}$ (ml)	⟨[NaCl]$^{\rm drop}$⟩ (M)			
88.9	5.0	1.73 (1)	1.91 (2)	1.74	1.59
99.1	3.5	1.68 (1)	1.87 (1)	1.69	1.55
109.2	2.1	1.64 (2)	1.83 (1)	1.65	1.51
119.4	0.7	1.59 (2)	1.78 (1)	1.60	1.47

dilution of the reservoir would be only about one part in a thousand, well beyond our ability to measure the change by refractometry.

4. The second experimental set

Four groups of tubes, with six replicate tubes per group, were prepared as described, with varying volumes of reservoir solution surveying four values of the droplet–reservoir separation ranging from 88.9 to 119.4 mm. Two equilibration durations, of 120 and 168 h, were examined. All of the procedures for deposition and harvesting of droplets employed in the first set of experiments were again employed for the second set. In particular, the initial volume and concentration of the droplet and the concentration of the reservoirs were the same. However, the average temperature in the thermal enclosure was 297.4 ± 0.5 K, about 1.5 K higher than the average temperature for the first experimental set.

The results of the experiments are given in Table 2. The averaged values of the NaCl concentration in the droplets for the four droplet–reservoir separations and two equilibration durations are over the six replicate experiments per group. There were no tape seal failures in these experiments. In Fig. 3 the average concentration of NaCl in the droplet is shown as a function of droplet–reservoir separation, at the two fixed times of equilibration. It is clear that the rate of equilibration is continuing to decrease with droplet–reservoir distance.

The two sets of experiments are each internally consistent but amalgamation of the two requires some first-order corrections. Focusing on the 121 h experiment from the first set and the 120 h experiment from the second set we first take into account that the first set was allowed to equilibrate for 1 h longer. Examination of Fig. 2(*b*) indicates that for longer droplet–reservoir separations the equilibration rate is approximately constant so we may apply a correction of 121/120 to the 120 h results from the second set to obtain estimates for a 121 h equilibration, Table 2. Because the average temperature of the second set was higher we expect the equilibrations to have been faster. In both the Fowlis *et al.* and Mikol *et al.* models, the effect of temperature enters principally through the dependence of the equilibration rate on the vapor pressure of the pure solvent. For pure water the vapor pressures at 295.9 and 297.4 K are 20.69 and 22.65 mm Hg, respectively. As the droplet equilibration rate is directly proportional to the vapor pressure, we therefore apply a correction of 20.69/22.65 to the 120 h results from the second set, already corrected to 121 h equilibration time. The composite graph of average NaCl concentration in the droplet, at 295.9 K and 121 h equilibration, *versus* droplet–reservoir separation over the entire range to $\sim$120 mm is shown in Fig. 4. The smoothness of the curve through the extrapolated data from the second set of experiments suggests that the first-order corrections for duration and temperature differences are reasonable.

As is clearly shown in Fig. 2(*b*) the rate of water equilibration in hanging-drop experiments is not constant over the course of the equilibration. It is a maximum at the start of the experiment and it drops to zero at full equilibration. The instantaneous rate of equilibration at the start of the experiment can be estimated from the earliest values of the average NaCl concentration. For the shortest droplet–reservoir distance examined the instantaneous rate of equilibration is (1.48–1.00) *M* NaCl/20 h = +0.024 (*M* NaCl) h^{-1}. For the longest distance examined the instantaneous rate of equilibration, assuming the rate is constant to 121 h, see Fig. 2(*b*), is (1.47–1.00) *M*/121 h = 0.00039 (*M* NaCl) h^{-1}, a factor of 6.2 slower, for the particulars of the experiment described, and corrected to a common temperature of 295.9 K.

5. Comparison with theory

Analytical expressions for the time to reach a particular point in the vapor-diffusion equilibration were developed by Fowlis *et al.* for the case of a droplet in the shape of a spherical cap and a concentric reservoir, Fig. 5(*a*); and by Sibille *et al.* for the case of a droplet in the shape of a right circular cylindrical plug and a similarly shaped reservoir, Fig. 5(*b*). Our experimental arrangement, Fig. 5(*c*), can be viewed as a hybrid of the two. The experimental droplet closely resembles the idealized spherical cap of the Fowlis *et al.* model while the experimental reservoir closely resembles the idealized right circular cylindrical plug of the Sibille *et al.* model. We sought to adapt, by minor modifications, either the Fowlis *et al.* or the Sibille *et al.* model to our experimental results.

The limiting behaviors of the two models in the case of large droplet–reservoir surface distances differ substantially. The Fowlis *et al.* model predicts a saturation limit; *i.e.*, a droplet–reservoir separation beyond which any further increase in the separation has negligible effect on the rate of water vapor equilibration. In comparison, the Sibille *et al.* model predicts a monotonic decrease in the equilibration rate with increasing droplet–reservoir separation, for all values of that separation, with no saturation limit. In view of the

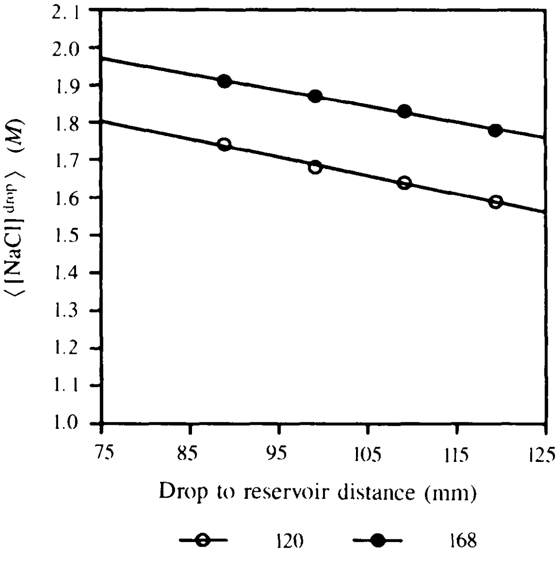

Fig. 3. Results of the second set of equilibration experiments, at 297.4 ± 0.5 K. The initial conditions are the same as those for the first set of experiments. The average sodium chloride concentration in the droplet is plotted as a function of the droplet–reservoir distance for two equilibration durations of 120 and 168 h.

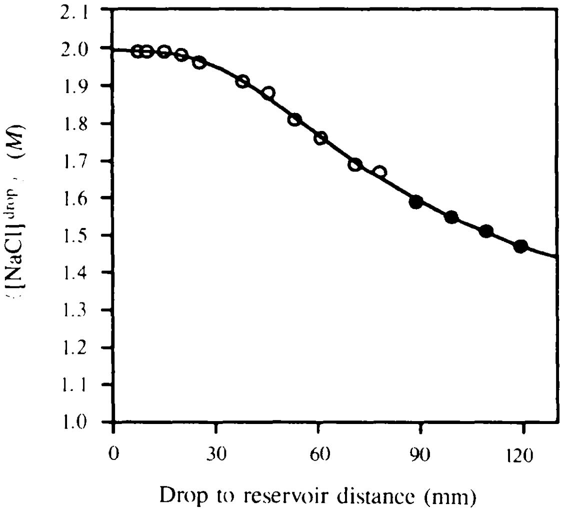

Fig. 4. The average concentration of NaCl in the droplet as a function of the distance from the droplet to the reservoir surface, after 121 h at 295.9 K. The initial conditions are 24 µl droplets of 1.00 *M* NaCl and reservoirs of 2.00 *M* NaCl. The first 11 points (o) of the graph are directly from the first set of experiments. The last four points (●) are from the second set of experiments after correction for the duration of the equilibration and the temperature difference between the two sets. The corrections are described in the text.

results of our second set of experiments, conducted at large droplet–reservoir separations, it is clear that the Sibille *et al.* model is the appropriate one to adapt to our data.

In the Sibille *et al.* formalism the elapsed time, t, to reach a particular point in the equilibration process is related to the difference, $\Delta_{H_2O}(t) = n^d_{H_2O}(t) - n^r_{H_2O}(t)$ between the number of moles of water in the drop at time t, $n^d_{H_2O}(t)$ and the number of moles of water in the reservoir at time t, $n^r_{H_2O}(t)$. The equilibration chamber is sealed against loss of water so $n^{tot}_{H_2O}(t) = n^d_{H_2O}(t) + n^r_{H_2O}(t) = 2n^d_{H_2O}(t) - n^{tot}_{H_2O}$ is a constant independent of time. Thus, we may write,

$$\Delta_{H_2O}(t) = n^d_{H_2O}(t) - n^r_{H_2O}(t) = 2n^d_{H_2O}(t) - n^{tot}_{H_2O}. \quad (1)$$

The solute, sodium chloride, is involatile so the difference $\Delta_{NaCl} = n^d_{NaCl} - n^r_{NaCl}$ and the sum $n^{tot}_{NaCl} = n^d_{NaCl} + n^r_{NaCl}$, where n^d_{NaCl} and n^r_{NaCl} are the number of moles of salt in drop and reservoir respectively, are constant; *i.e.*, independent of time.

Vapor-pressure equilibrium is reached asymptotically as $t \to \infty$ and the equilibrium value of $\Delta_{H_2O}(t)$ as $t \to \infty$ is given by,

$$\lim_{t \to \infty} \Delta_{H_2O}(t) \equiv \Delta_{H_2O}(\infty) = \Delta_{NaCl}(n_{H_2O}/n_{NaCl}). \quad (2)$$

The theory is simplified by the introduction of two dimensionless quantities,

$$\delta_{H_2O}(t) = \Delta_{H_2O}(t)/\Delta_{H_2O}(0), \quad (3)$$

and

$$\delta_{H_2O}(\infty) = \Delta_{H_2O}(\infty)/\Delta_{H_2O}(0), \quad (4)$$

where $\Delta_{H_2O}(0)$ is the initial value of $\Delta_{H_2O}(t)$. Expressed in terms of these parameters, the time t to reach a particular stage in the equilibration process is given by,

$$t/\tau = \{[\delta^2_{H_2O}(t) - 1]/2\} + \delta_{H_2O}(\infty)[\delta_{H_2O}(t) - 1] + (\delta^2_{H_2O}(\infty) - \{(n^{tot}_{H_2O})^2/[\Delta_{H_2O}(0)]^2\}) \times \ln\{[\delta_{H_2O}(t) - \delta_{H_2O}(\infty)]/[1 - \delta_{H_2O}(\infty)]\}, \quad (5)$$

where τ is a characteristic time given by,

$$\tau = RTh[\Delta_{H_2O}(0)]^2/(4S_{eff}D_{H_2O}P^0_{H_2O}W_{NaCl}n^{tot}_{NaCl}). \quad (6)$$

Terms appearing in (6) include: R, the gas law constant; T, the absolute temperature; h, the distance between the surface of the reservoir solution and the support surface for the droplet; S_{eff}, the effective surface area of the reservoir solution; D_{H_2O}, the diffusion coefficient of water in air at temperature T and one atmosphere; $P^0_{H_2O}$, the vapor pressure of pure water at temperature T; and W_{NaCl}, the vapor-pressure lowering coefficient for salt in aqueous solution. When both drop and reservoir have cylindrical geometry, $S_{eff} = S$, the geometrical cross-section of the cylinder. As we will show in the sequel, a quantitative fit to the time course data in Table 1 results by letting S_{eff} be a function of h.

While the Sibille *et al.* model is compactly expressed in terms of moles of water and salt, all of our experimental results are in terms of molar concentrations of salt in aqueous solution. These include the initial concentrations of salt in the droplet, $C^d_{NaCl}(0)$, and concentrations at times t, $C^d_{NaCl}(t)$; the initial volume of the drops, $V^d(0) = 24\,\mu l$; and the concentration and volume of the reservoir, $C^r_{NaCl}(t)$ and $V^r(t)$, both of which are to a good approximation time invariant. From these data $n^{tot}_{NaCl} = n^d_{NaCl} + n^r_{NaCl}$ and $\Delta_{NaCl} = n^d_{NaCl} - n^r_{NaCl}$ were computed using $n^d_{NaCl} = V^d(0)/C^d_{NaCl}(0)$ and $n^r_{NaCl} = V^r(0)/C^r_{NaCl}(0)$. The volume of the drop at any time, t, was computed as $V^d(t) = n^d_{NaCl}/C^d_{NaCl}(t)$. The value of $n^d{}_{H_2O}(t)$ at time t was computed as,

$$n^d_{NaCl}(t) = [V^d(t) - n^d_{NaCl}\bar{V}_{NaCl}]/\bar{V}_{H_2O}, \quad (7)$$

where $\bar{V}_{H_2O} = 0.018010$ liter mol^{-1} is the partial molar volume of water and $\bar{V}_{NaCl} = 0.019938$ liter mol^{-1} is the partial molar volume of salt. These partial molar volumes were determined from an analysis of the density of aqueous sodium chloride (Weast & Lide, 1990) using the method of apparent molar volumes (Daniels *et al.*, 1970). The number of moles of water in the reservoir, $n^r_{H_2O}(0)$, was computed as,

$$n^r_{H_2O}(0) = [V^r(0) - n^r_{NaCl}\cdot\bar{V}_{NaCl}]/\bar{V}_{H_2O}. \quad (8)$$

With the above results $n^{tot}_{H_2O} = n^d_{H_2O}(0) + n^r_{H_2O}(0)$ was computed using (7) and (8), while $\Delta_{H_2O}(t)$ was computed at times t using (1) and (7). With $n^{tot}_{H_2O}$, $\Delta^{tot}_{H_2O}(t)$, $\Delta_{H_2O}(0)$, n^{tot}_{NaCl} and Δ_{NaCl} thus evaluated terms,

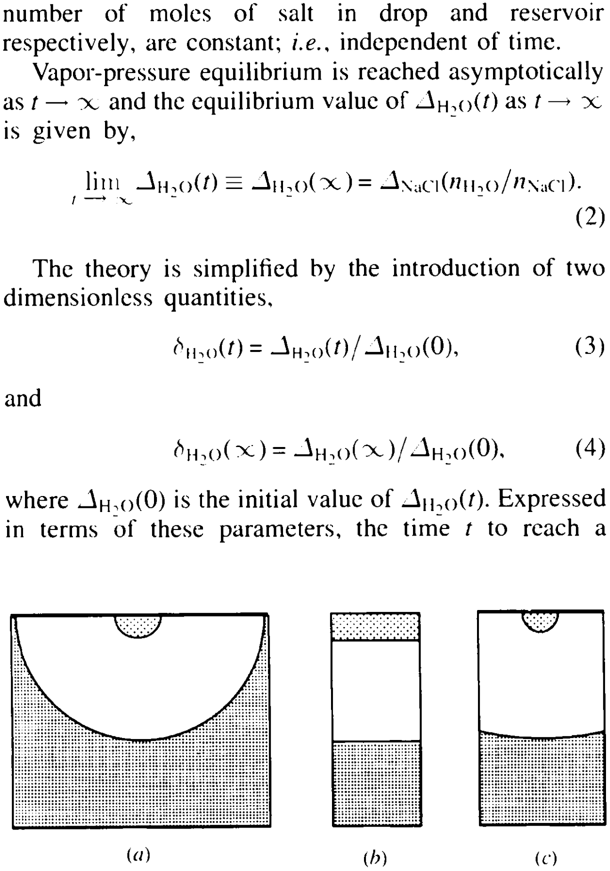

Fig. 5. Idealized hanging-drop vapor-diffusion models. (*a*) Fowlis *et al.* model assumes that the droplet is a spherical cap and that the reservoir is concentric with the droplet. In the case of a hemispherical drop the reservoir surface is supposed to be hemispherical as well. (*b*) The Sibille *et al.* model of the Plaas-Link tube. Both the droplet and the reservoir are supposed to be right circular cylindrical plugs. (*c*) Our experimental arrangement. The geometry of the droplet is well approximated by the Fowlis *et al.* droplet, while the geometry of the reservoir is well approximated by the Sibille *et al.* reservoir.

$\Delta_{H_2O}(\infty)$, $\delta_{H_2O}(t)$ and $\delta_{H_2O}(\infty)$ were computed using (2), (3) and (4). Thus all of the terms on the right-hand side of (5), at the various values of the time t, could be evaluated.

The characteristic time τ in (6) was evaluated as follows. As indicated, h in the original theory is the distance between the surfaces of the 'droplet' and 'reservoir', each approximated as right circular cylindrical plugs of liquid. In the experimental arrangement here the surface to surface distance is ill defined and time dependent so we adopt the Fowlis *et al.* definition for the droplet–reservoir distance. In the case of hemispherical droplets that distance is measured from the bottom of the meniscus, Fig. 1, to the support for the droplet. The values for (0.26 cm^2 s^{-1}) and $P^0_{H_2O}$ (0.027721 atm at $T = 295$ K) are from Cussler (1984) and from Weast & Lide (1990), respectively. The vapor pressure lowering coefficient, $W_{NaCl} = 1.875$, was evaluated by the method of Fowlis *et al.* using the osmotic coefficient data of Clarke & Glew (1985) for NaCl, and the relationship (Lewis & Randall, 1961) $P_{H_2O}(m) = P^0_{H_2O}[-2m\varphi(m)/55.51]$ where m is the molality of NaCl, $P_{H_2O}(m)$ is the vapor pressure of water at a particular molal concentration of NaCl, and $\varphi(m)$ is the osmotic coefficient.

The only remaining unknown in (6) is S_{eff}, the effective cross-sectional area of the reservoir. In treating the Plaas-Link tube geometry, Fig. 5(*b*), the effective cross-section is taken as the geometrical cross-section of the tube; *i.e.*, the actual cross-section of the right circular cylindrical drop and reservoir solutions. Here we treat S_{eff} as a parameter to be fitted, by least squares, to the observed kinetics data measured in the first set of experiments. For each fixed value of h, a value of S_{eff} that best fits (5) to the values of $\langle[\mathrm{NaCl}]^{\mathrm{droplet}}\rangle$ for the six times t, spanning 20–121 h, was evaluated. Five example fits (of the 11 experiments comprising the first set) are shown in Fig. 6. Note that for each time course a different value of S_{eff} was fitted, but for each set of six data points only a single variable was adjusted to pass the curve calculated from (5) and (6) through the points. The values of S_{eff} for the 11 experiments in the first set are shown as a function of h in Fig. 7. As h increases the value of S_{eff} increases, asymptotically approaching the geometric cross-section in the limit of large droplet–reservoir separation.

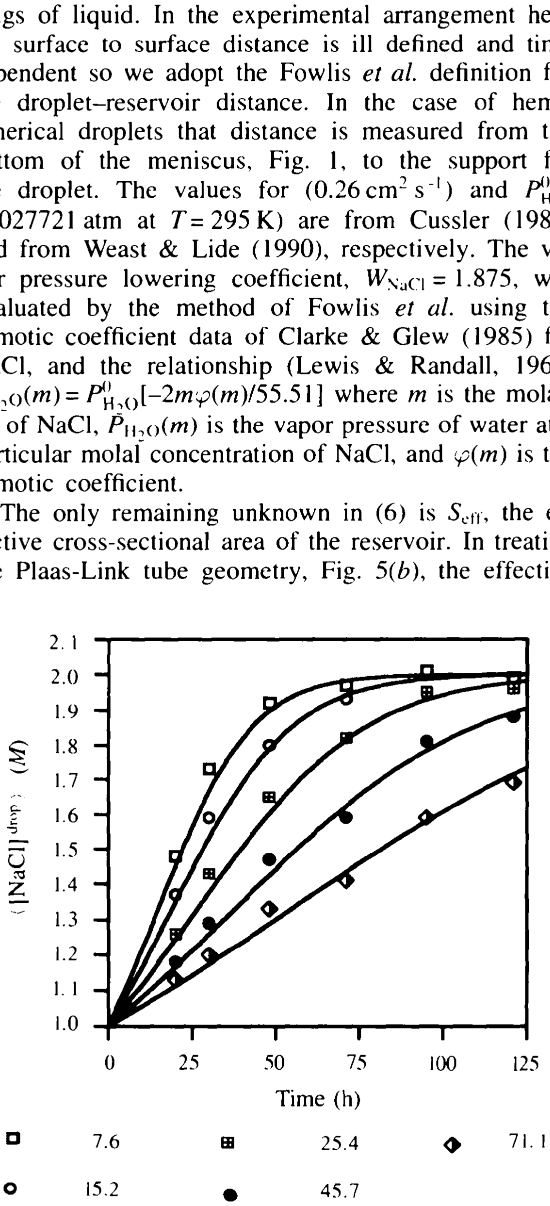

Fig. 6. Examples of the fits of the modified Sibille *et al.* model, (5) and (6), to the data from the first experimental set. Shown are curves fit through five of the 11 subsets of data (other fits not shown for the sake of clarity). Each curve was fit by adjusting a single parameter, S_{eff}, in the model to account for the difference in the hypothetical (Fig. 5*b*) and actual (Fig. 1) geometrical arrangement of droplet and reservoir. There were six data points available for fitting S_{eff} at each value of h, the droplet–reservoir separation. These curves should be compared directly with those in Fig. 2(*b*).

6. Discussion

In accord with the principal assumption of Fowlis *et al.* and Sibille *et al.*, the rate of equilibration in hanging-drop crystallization experiments depends upon the distance from the reservoir to the droplet. From a theoretical point of view it is important to note that these results are supportive of the contention that the rate-limiting step in vapor diffusion is transit of water across the vapor space. Recent studies by DeTitta & Luft (1995) have shown that the rate of equilibration in sitting-drop experiments

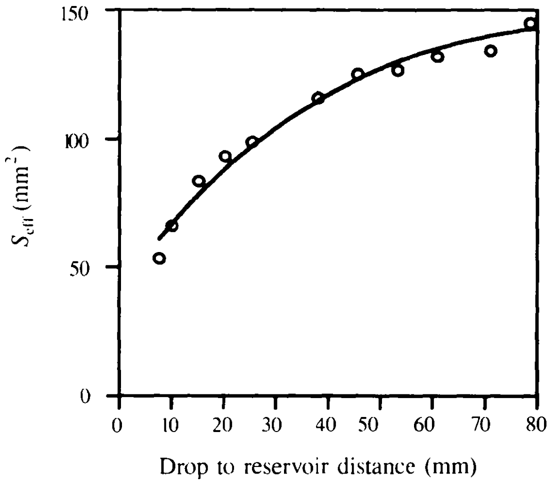

Fig. 7. Graph of the effective surface area of the reservoir, S_{eff}, *versus* the droplet–reservoir distance, h. The 11 points correspond to the 11 droplet–reservoir separations examined in the first experimental set, Table 1. The values of S_{eff} are those that best fit the time courses shown in Figs. 2(*b*) and 6. In the limit of large droplet–reservoir separation the effective cross-section approaches the geometric cross-section, suggesting that the model is appropriate to the experiment and that, at large separations, the shape of the droplet becomes unimportant with respect to water vapor equilibration kinetics. The geometric cross-section is 145 mm^2.

is sensitive to the residual pressure of air in the vapor chamber, which is also in accord with this hypothesis.

With very minor modifications, the model developed by Sibille *et al.* for the Plaas-Link tube has been adapted to our experimental protocol with its substantially different geometric arrangement of droplet and reservoir. The fact that $S_{\rm eff}$ in the modified theory approaches the geometric value of the reservoir cross-sectional area, in the limit of large droplet–reservoir separations, suggests that the Sibille *et al.* model is an appropriate one for this arrangement of droplet, vapor space and reservoir. It also suggests that the shape of the droplet and its consequent effect on the rate of water equilibration, as described by Fowlis *et al.*, becomes less and less important as the droplet–reservoir separation increases. At separations greater than ~80 mm the shape of the droplet appears not to affect the kinetics, as the observed rate of equilibration for our hemispherical droplet is equal to the calculated rate of equilibration for a disc-shaped droplet of cross-sectional area equal to that of the reservoir. Based on these observations we suggest that, for a geometric arrangement of droplet and reservoir as shown in Fig. 1, at small values of the droplet–reservoir separation (such as in Linbro plate equilibrations) the mathematical treatment of Fowlis *et al.* can be employed; at large values, the original treatment of Sibille *et al.* can be employed; and at intermediate values, such as those reported here, our modified treatment of Sibille *et al.* can be employed.

From the point of view of crystal growth, it is not the rate of water equilibration per se that is of primary importance. Rather it is the rate at which supersaturation of the macromolecule develops that determines the outcome of the crystal growth experiment. The two rates are intimately but not simply related. Referring to the two-dimensional solubility diagram of Riès-Kautt & Ducruix (1992), the solubility curve is the locus of points at which the protein concentration at the solubility limit is plotted against the crystallizing agent concentration. Trajectories of conditions within the droplet radiate out from the origin of the diagram and intersect the solubility curve at various angles, Fig. 8. For some trajectories a small change in the rate of water equilibration can lead to a large change in the rate at which supersaturation develops. Under these circumstances a variation of the reservoir volume, intended or otherwise, may lead to inconsistent crystallization results.

From the standard deviations given in Tables 1 and 2 it is clear that, when droplets and reservoirs are each identically constituted, each with uniform volumes, with a fixed distance separating them, and when allowed to equilibrate at the same temperature, ordinary care in the preparation of the experiments leads to very little variation in the rate of equilibration. As the rate of equilibration in macromolecular crystallization can have a profound effect on the quality and size of crystals (Feher & Kam, 1985), any protocol designed to optimize crystal growth outcome (Carter & Yin, 1994) should be highly reproducible. Based on our observations, vapor diffusion fits that requirement. The equilibrations examined here employed droplets of uniform chemical composition. We would anticipate more variability in our results had we constituted droplets according to the frequently prescribed recipe of diluting equal volumes of macromolecular stock solution and reservoir solution. Additionally, temperature variations must be strictly minimized in order to achieve consistent results.

Finally, it appears that variation of the droplet–reservoir separation affords the crystal grower a means to optimize the rates at which supersaturation, nucleation and crystal growth occur. Like the Z/3 plate technology (Luft *et al.*, 1994; Arakali, Easley, Luft & DeTitta, 1994) the technique that we describe above is fully passive; *i.e.*, once set up, it requires no

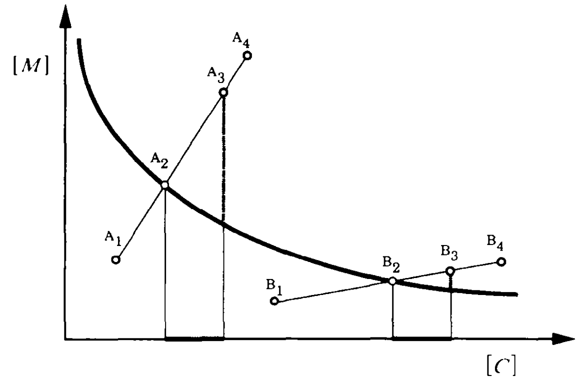

Fig. 8. Schematic relationship between the rate at which water leaves the droplet and the rate at which supersaturation of the macromolecule in the droplet develops. Shown is a two-dimensional solubility diagram in which the concentrations of macromolecule, $[M]$, and crystallizing agent, $[C]$, form the ordinate and abscissa of the graph, respectively (Riès-Kautt & Ducruix, 1992). The solubility curve (bold line) is the locus of points defining the solubility concentration of the macromolecule at every value of the crystallizing agent concentration. Shown are two potential trajectories for vapor-diffusion crystallizations. Note that both trajectories extrapolate back to the origin as they must for vapor-diffusion experiments involving only one volatile component. The trajectory $A1 \rightarrow A4$ represents an experiment in which the concentration of crystallizing agent is always relatively low, therefore the concentration of macromolecule must always be relatively high. The trajectory $B1 \rightarrow B4$ represents the opposite strategy. Points A_1 and B_1 represent initial conditions in the droplets. Where the trajectories intersect the solubility curve, A_2 and B_2, $[M]$ equals the solubility concentration $[M]^{\rm sol}$ and by definition the supersaturation $\sigma = [M]/[M]^{\rm sol} = 1$. We suppose that over the two trajectories $\Delta[C]/\Delta t$ is approximately constant. By variation of the droplet–reservoir distance we can contrive to adjust the rates of water equilibration for the two experiments to be equal; *i.e.*, for $\Delta[C]/\Delta t$ to be equal. In unit time conditions in the droplets evolve from A_2 to A_3 and from B_2 to B_3. Note that for trajectory A both $\Delta[M]$ and $\Delta\sigma$ are large while for trajectory B both $\Delta[M]$ and $\Delta\sigma$ are small. A small variation in $\Delta[C]/\Delta t$ such as might result from the inadvertent variation of the reservoir volume, can have a large effect on the rate at which supersaturation develops in trajectory A, while in trajectory B the rate of supersaturation might be rather insensitive to such variations.

further intervention on the part of the crystal grower. Furthermore, the technique described is very simple to set up, leads to highly reproducible results, and involves inexpensive, readily available materials. Additionally the tape support for the drop and seal for the reservoir makes manipulation of the droplet very simple. Once crystals are grown, the washer provides both a lever to gently break the reservoir seal and a natural protection for the crystals and droplet. The washer can be sealed with a second piece of tape on the open side, facilitating storage and transportation of the droplet containing crystals. Provided the unit is not vigorously disturbed, the droplet will not move from its place nor evaporate through the tape seals.

We wish to thank Drs Madeleine Riès-Kautt, CNRS Gif-sur-Yvette and Robert Blessing for their many helpful criticisms, Dr Vivian Cody for partial support of this work, Jennifer Yadav for help with the second set of experiments, and Adele K. DeTitta for help with part of the first set of experiments. Preliminary investigations of the effect of the droplet–reservoir separation were carried out with the help of Dr Catherine Hansen. This work is dedicated to the memory of George R. DeTitta (1920–1994) and was supported in Buffalo by NIH Grants GM46733 and DK41009, American Cancer Society Grant NP-826, and NASA Grant NAG8-1152; and in Huntsville by NIH Grant GM51018 and by the UAH Consortium for Materials Development in Space, funded by NASA Grant NAGW-812.

References

Arakali, S. V., Easley, S., Luft, J. R. & DeTitta, G. T. (1994). *Acta Cryst.* D**50**, 472–478.

Arakali, S. V., Luft, J. R. & DeTitta, G. T. (1995). *Acta Cryst.* D**51**, 772–779.

Boistelle, R. & Astier, J. P. (1988). *J. Cryst. Growth*, **90**, 14–30.

Carter, C. W. & Yin, Y. (1994). *Acta Cryst.* D**50**, 572–590.

Clarke, E. C. W. & Glew, D. N. (1985). *J. Phys. Chem.* **14**, 489.

Daniels, F., Alberty, R. A., Williams, J. W., Cornwell, C. D., Bender, P., & Harriman, J. E. (1970). *Experimental Physical Chemistry*, pp. 95–100. New York: McGraw-Hill.

Cussler, E. L. (1984). *Diffusion-Mass Transfer in Fluid Systems.* Cambridge University Press.

DeTitta, G. T. & Luft, J. R. (1995). *Acta Cryst.* D**51**, 786–792.

Ducruix, A. & Giegé, R. (1992). *Crystallization of Nucleic Acids and Proteins – A Practical Approach.* Oxford: IRL Press/Oxford University Press.

Feher, G. & Kam, Z. (1985). *Methods Enzymol.* **114**, 77–112.

Fowlis, W. W., DeLucas, L. J., Twigg, P. J., Howard, S. B., Meehan, E. J. & Baird, J. K. (1988). *J. Cryst. Growth*, **90**, 117–129.

Lewis, G. N. & Randall, M. (1961) *Thermodynamics*, revised by K. S. Pitzer & L. Brewer, 2nd ed., pp. 246, 321. New York: McGraw-Hill.

Luft, J. R., Arakali, S. V., Kirisits, M. J., Kalenik, J., Wawrzak, I., Cody, V., Pangborn, W. A. & DeTitta, G. T. (1994). *J. Appl. Cryst.* **27**, 443–452.

Luft, J. R., Cody, V. & DeTitta, G. T. (1992). *J. Cryst. Growth*, **122**, 181–185.

Luft, J. R. & DeTitta, G. T. (1992). *J. Appl. Cryst.* **25**, 324–325.

McPherson, A. (1982). *Preparation and Analysis of Protein Crystals.* New York; John Wiley/Malabar, FL: Krieger Publishing Co.

Mikol, V., Rodeau, J.-L. & Giegé, R. (1990). *Analyt. Biochem.* **186**, 332-339.

Morris, D. W., Kim, D. Y. & McPherson, A. (1989). *Biotechniques*, **7**, 522–527.

Plaas-Link, A. & Cornier, J. (1988). *Appl. Microgravity Tech.* **3**, 123–132.

Riès-Kautt, M. & Ducruix, A. (1992). *Crystallization of Nucleic Acids and Proteins - A Practical Approach.* Oxford: IRL Press/Oxford University Press.

Sibille, L., Clunie, J. C. & Baird, J. K. (1991). *J. Cryst. Growth*, **110**, 80–88.

Weast, R. C. & Lide, D. R. (1990). *CRC Handbook of Chemistry and Physics*, pp. D-255–D-256. Boca Raton, FL: CRC Press.